The Effect of Surfactant Chain Length and Type on the Photocatalytic Activity of Mesoporous TiO_2 Nanoparticles Obtained via Modified Sol-Gel Process

Kachbouri, Sana; Elaloui, Elimame•

Material Environment and Energy Laboratory (UR14ES26), Faculty of Sciences of Gafsa, University of Gafsa, TUNISIA

Moussaoui, Younes*+•

Organic Chemistry Laboratory (LR17ES08), Faculty of Sciences of Sfax, University of Sfax, TUNISIA

ABSTRACT: *Mesoporous amorphous and nanocrystalline titanium dioxide were prepared by simple and environmental friendly modified Sol-Gel method using cationic (C_{14}TAB, C_{16}TAB, C_{18}TAB) and nonionic (Plantacare UP K55) surfactant as pore forming agent. The obtained particles were characterized by BET, TEM, FT-IR and XRD techniques. The effect of cationic surfactant chain length and type of template on the photocatalytic activity of as prepared TiO_2 nanoparticles were investigated by the degradation of rhodamine B in water solution under UV irradiation. The results indicated that this process was well described by the pseudo-first order kinetic model. All the prepared titanium dioxide particles with cationic and nonionic surfactant exhibited higher performance for rhodamine B photo-degradation. The sample with large pore size and small particle size which obtained by using C_{18}TAB surfactant showed high photocatalytic activity compared with the others samples and commercial P25. The mechanism of photocatalytic degradation of rhodamine B was proposed based on the degradation products determined by GC/MS and LC/MS. The performance of the recycled TiO_2 as photocatalyst was investigated.*

KEYWORDS: *Sol-gel processes; Mesoporous materials; Reaction mechanisms; Photochemistry; Nanostructures.*

INTRODUCTION

Titanium dioxide is one of the most important nanomaterials which have been used in the areas of pigments, biomedical materials, catalysts and supports, dielectric materials, gas sensors, waste water purification, dye- sensitized solar cells and photo-catalysts [1-8]. Nanostructured TiO_2 with significant properties like defined morphology; very fine size and single crystalline phase, have been prepared by a variety of techniques such as solvothermal process [9-12], hydrothermal [13-16], mechanochemical [17], anodization process [18] and

***** *To whom correspondence should be addressed.*

+ E-mail: y.moussaoui2@gmx.fr

• Other Address: Faculty of Sciences of Gafsa, University of Gafsa, TUNISIA

1021-9986/2019/1/17-26 10/$/6.00

sol-gel method [2,19]. The sol–gel method has proven to be a very useful tool for the preparation of dispersed nanoparticles TiO_2 because of its ease of operation and low processing cost [19]. The sol-gel process offers many advantages to producing materials with high homogeneity, purity and possibility to control the composition and micro structure, while varying parameters such as the concentration of alkoxide precursor of titanium, the molar ratio of titanium/water, nature of the solvent, catalyst, and conditions of calcinations [19-22]. Currently, mesoporous titania nanoparticles obtained via modified sol-gel process using surfactant as directing and pore forming agent, have attracted much attention as photo-catalyst, as they are considered to be more applicable in practice than titania films because of its large surface area and porous frameworks [1, 23-26]. In fact it's known that in case of using water as solvent with large excess, hydrolysis process proceeds very rapidly and thereafter provides fine particles witch agglomerated very quickly, giving large aggregates with micrometer size. So in order to overcome this issue, the use of surfactants makes it possible to obtain particles with small size and defined shape. To date, a variety of hard and soft templates have been applied to direct the formation of mesoporous titania spheres. In 1995, *Antonelli* and *Ying* [27] reported the synthesis of mesoporous TiO_2 through modified sol-gel route in the presence of alklyphosphate surfactant templates. Anatase TiO_2 nanospheres have been prepared by *Yang* and *Zeng* [28] via Ostwald ripening after a longer hydrothermal treatment. *Ren et al.* [29] have prepared hollow microspheres of mesoporous TiO_2 adopting the surfactant-assisted method. Most of , titanium nanoparticles already synthesized and reported in the literature have been used as photocatalyst for dye degradation. In spite of the lots of work focusing on semiconductors employed for the degradation of hazardous materials such as nanocomposites [30], TiO_2 nanoparticles still more suitable for industrial use due to its high stability and low cost.

Recently, *Bakre et al.* [31] reported the influence of acid chain length (formic acid, acetic acid, butyric acid, octanoic acid, and palmitic acid) on the properties of TiO_2 prepared by sol-gel method for the degradation of methylene blue. However, a comparative study to emphasize the effects of alkyl chain length or type of surfactant on the photodegradation of organic dyes has not been yet reported. In this regard, the main objective of this study is to investigate the effect of cationic and nonionic surfactant in the process of photocatalytic decomposition of a model dye.

To sum up, this research describes a facile, simple and inexpensive route to synthesize mesoporous amorphous TiO_2 nanoparticles with high surface area and large pore size using two types of surfactants (cationic and nonionic) as pore forming agent and solvent extraction method to remove templates in the preparation process. In fact, these templates were used by mixing them in water in order to obtain micelles and thereafter increasing the porosity within the nanoparticle. Thus, three cationic surfactants of alkyl chains C_nTAB (n = 14, 16 and 18) of n-alkyl ammonium bromide have been chosen to study the influence of chain length on photodegradation. It has been adopted that the cationic surfactant C_nTAB provided a favorable organophilic environment to the hydrolysis and condensation of Ti and could be completely removed without disrupting the photocatalytic activity [32]. As nonionic surfactant, a sugar surfactant, Alkylpolyglucoside (Plantacare K55) have been chosen because it was green and environmental friendly surfactant witch considered as attractive amphiphilic molecules for constructing aggregates. Besides, it was a good gelator for various solvents because it could easily form hydrogen-bonding networks and solvophobic interactions of tail chains [33]. To our knowledge, there is no literature about the use of sugar surfactant type on the synthesis of TiO_2 nanoparticles. Then, after thermal treatment to provide anatase phase, this mesoporous TiO_2 themselves will be better photo-catalytic carriers for degradation of rhodamine B dye which was one of the most famous xanthenes dye and dye organic pollutants due to its good stability as a dye laser material. We investigated the effect of chain length and type of surfactant on the photocatalytic activity of mesoporous titania nanoparticles.

EXPERIMENTAL SECTION

Chemicals

Titanium (IV) butoxide (97%), tetradecyltrimethyl ammonium bromide ($C_{14}TAB$), the work of the lot bromide ($C_{16}TAB$) and octadecyltrimethyl ammonium bromide ($C_{18}TAB$) were purchased from Sigma-Aldrich. Alkylpolyglucoside (Plantacare UP K55) from Cognis. Absolute ethanol (>99.7%, Merck),

and Milli-Q water (18.2 MΩ cm) were used for the synthesis. Rhodamine B (RhB) (97%) from Sigma-Aldrich was used for photo-catalysis activity. Commercial P25 TiO_2 powder (80% anatase, 20% rutile) from Degussa was used for the comparison of the photocatalytic activity.

Preparation of mesoporous TiO_2 photo-catalyst

In a typical preparation process of mesoporous amorphous TiO_2, 200mg of surfactant (C_{14}TAB, C_{16}TAB, C_{18}TAB and Plantacare UP K55 for samples TP1, TP2, TP3, and TP4 respectively) and 60 mL of water were mixed under constant stirring at 40°C during 2 h until dissolution. Then, 1 mL of titanium butoxide was dissolved in 20 mL of absolute ethanol and was added to the above solution drop wise under vigorous stirring at 40°C. Then a milky white suspension (sol) formation was observed immediately. The milky white solution was kept 12 h in stirring at room temperature (28-30°C) and then collected by centrifugation for 15 min at 5.000 rev/s. Subsequently, the sample was extracted with an alcoholic solution of NH_4NO_3 (6 g/L) using sonication for 30 min at 25°C followed by intermittent washing with water and ethanol three times to remove surfactant.

In order to obtain amorphous TiO_2 nanoparticles, the resulted precipitate was dried at 80°C for 1 h to evaporate water and organic material to the maximum extent. Finally, to obtain desired TiO_2 nanocrystalline for photocatalytic applications, the dried powders obtained were calcinated at 450°C.

Characterization

The particle size and morphology of the powder were observed by Transmission Electron Microscope (TEM) using a JEOL 1200 EX II.

Specific surface areas (BET measurements) were determined using a Micromeritics ASAP-2020 apparatus based on N_2 adsorption. The crystallographic phases of TiO_2 were identified from X-Ray Diffraction (XRD) patterns recorded with a Philips PANALYTICAL X'pert MPD using Cu $K_{\alpha 1}$ radiation (λ_{Cu}=1.5406 Å).

Photo-catalytic degradation experiments

The photo-catalytic activity of mesoporous TiO_2 nanoparticles was evaluated by the degradation efficiency of RhB. 200 mg of photo-catalyst was dispersed in an aqueous solution of RhB (100 mL, 20 mg/L). The suspension was magnetically stirred in dark for 60 min to reach adsorption/desorption equilibrium of RhB molecules on the surface of the photo-catalyst. Then, the suspension was irradiated using two UV lamps at 366 nm. The progress of the degradation of RhB was monitored every 5 min for subsequent target dye concentration analysis after filtration through Millipore syringe filter of 0.20 μm. The degradation efficiency of RhB was evaluated by measuring the concentration of a centrifuged RhB solution at 554 nm which corresponds to the absorption maximum of RhB using a UV-vis spectrophotometer (DU-800, BeckMAN Coulter). The degradation efficiency and the decolorization efficiency of catalysts after various intervals of time can be calculated using the following equations:

$$\text{degradation efficiency}(\%) = \frac{A_0 - A_t}{A_0} \times 100$$

Where A_0 and A_t are the initial absorbance and the absorbance after various intervals of time (t), respectively.

$$\text{decolorization efficiency}(\%) = \frac{C_0 - C_t}{C_0} \times 10$$

Where C_0 is the initial concentration of dye and C_t is the concentration of dye after photo-irradiation.

The intermediates were identified by GC/MS (Thermo-Trace GC Ultra with Quadrupole Spectrometer as a detector) and LC/MS (Thermo). 3 mL filtered solution was collected after every 3 min and then was extracted with 5 mL of dichloromethane three times, and the extracted solution was dehydrated using anhydrous sodium sulfate. Finally, 2 μL of extracted solution was automatically injected into GC with DB-5 column (fused-silica capillary column, 30 m × 0.25 mm ID of 0.25 μm film thickness with a 5% equivalent polysilphenylene-siloxane) using splitless mode. For LC/MS analysis, the samples were separated using a Beta Basic-C18 HPLC column (150 × 2.1 mm ID of 5 μm) at a flow rate of 0.2 mL/min, and the mobile phase was 60% methanol and 40% water.

RESULTS AND DISCUSSION

Characterization of amorphous and mesoporous TiO_2 nanoparticles

Sol-gel method of synthesizing nanomaterial is very popular amongst chemists and is widely employed to

prepare oxide materials. This method refers to the hydrolysis and condensation of alkoxide based precursor. The preparation of the TiO_2 nanoparticles can be effectively conducted through the hydrolysis and condensation of titanium alkoxides $Ti(OR)_4$ (where R is ethyl, *i*-propyl, *n*-butyl, etc) in aqueous media. These reactions can be schematically represented as follows:

$$Ti(OR)_4 + 4H_2O \rightarrow Ti(OH)_4 + 4ROH \quad (Hydrolysis)$$

$$Ti(OH)_4 \rightarrow TiO_2, xH_2O + (2-x)H_2O \quad (Condensation)$$

The hierarchical porous structure of TiO_2 is confirmed by its TEM images. The TEM image in Fig. 1 reveals a large amount of very small particles with the average size of about 50 nm and constitutes a disordered wormhole framework, which is a typical characteristic of mesoporous structure. It's obvious that the introduction of surfactant has a significant influence on the morphology of titania nanoparticles. It's shown that particles size decreases with addition of templates. The morphology of TiO_2 nanoparticles synthesized by Plantacare UP K55 (TP4), is similar to these synthesized with cationic surfactant, but it shows more defined spherical particles than the others (Fig. 1).

The surface area and porosity of the TiO_2 nanoparticles were investigated using the nitrogen adsorption and desorption isotherm. All particles are porous before calcination. Surfactants were removed by using extraction to keep the mesostructure and the amorphous phase, because it is difficult to keep the mesostructure after removing completely the structuring agent. The nitrogen adsorption-desorption isotherm shows a pure type IV adsorption according to the IUPAC classification [34] for all the TiO_2 samples. The late and steep adsorption step shows the relatively large pore size. In addition, isotherms show hysteresis loop of type H1 characteristic of mesopores.

As expected, the specific surface area increased with the increase in chain length of hydrophilic part of the template in the case of cationic alkylammonium bromide (Table 1). The plots of the pore size distribution are determined by the BJH (Barrett-Joyner-Halenda) method from the desorption branch of the isotherm, which shows that TiO_2 spheres after extraction have very obvious mesoporous structure. The average pore diameters of TiO_2 particles ranged from 8 to 9 nm (Table 1).

Characterization of crystalline TiO_2 nanoparticles

The as-synthesized amorphous TiO_2 nanoparticles can be transformed into the crystalline phase after calcination at 450°C. The crystal phase of the as-synthesized TiO_2 samples were detected by using X-Ray powder Diffraction (XRD). All diffraction peaks are well defined and it can be clearly observed in Fig. 2, that anatase is the main formed phase in the different experimental conditions. It's known that anatase TiO_2 nanoparticles were very photoactive and practical for water treatment and water purification.

The peaks located at 25.3, 37.8, 48.1, 54.0 respond to the (101), (004), (200), (105) and (211) planes of the anatase phase according to the JCPDS files (Joint Committee on Powder Diffraction Standards Card No: 21-1272). However, an additional peak at 2θ= 30.8 respond to the (121) in the patterns of samples TP1* and TP2* suggests the presence of a low amount of brookite. The XRD patterns were then analyzed using X'Pert High Score Plus program and the proportion of the different TiO_2 polymorphs, anatase, brookite or rutile in the solids can be determined from the quantitative method as shown by the following equations [35]:

$$W_A = \frac{K_A A_A}{K_A A_A + A_R + K_B A_B} \quad (1)$$

$$W_R = \frac{A_R}{K_A A_A + A_R + K_B A_B} \quad (2)$$

$$W_B = \frac{K_B A_B}{K_A A_A + A_R + K_B A_B} \quad (3)$$

Where W_A, W_B, and W_R represent the weight fraction of anatase, brookite, and rutile respectively. A_A, A_B, and A_R represent the integrated intensity of the anatase (101) peak, the brookite (121) peak and the rutile (110) peak respectively. The coefficients $K_A = 0.886$ and $K_B = 2.721$.

Samples TP1* and TP2* contains anatase and brookite, so the weight fraction of anatase (W_A) and brookite (W_B) can be calculated by removing the A_R coefficient (Table 2).

The broadening of the anatase diffraction peaks is attributed to the nanometer size of the particles and could be used to determine the crystallite size of the particles using the Debye–Scherrer's equation as follows [36]:

$$FWHM = \frac{K\lambda}{S\cos\theta}$$

Table 1: Physicochemical properties of mesoporous TiO_2 particles prepared with different surfactants.

Sample	surfactant	BET Surface Area (m^2/g)	Pore Size (nm)	Pore Volume (cm^3/g)
TP1	C_{14}TAB	437	8.5	1. 01
TP2	C_{16}TAB	467	9.9	0. 88
TP3	C_{18}TAB	508	8.1	1. 02
TP4	Plantacare K55	400	8.5	0. 89

Table 2: XRD particle size and Characterization results of N2 adsorption-desorption for crystallized TiO_2 samples and commercial P25.

Sample	XRD particle size (nm)	Crystalline composition (%A/%B/%R)	S_{BET} (m^2/g)	Pore size dp (nm)
TP1*	12.47	95% A+ 5%B	93. 6	8.7
TP2*	10.65	90% A+ 10%B	86.0	9.3
TP3*	10.51	100%A	104.0	10.2
TP4*	12.00	100%A	67.2	12.7
P25	21.00	20%R+ 80%A	56.0	17. 5

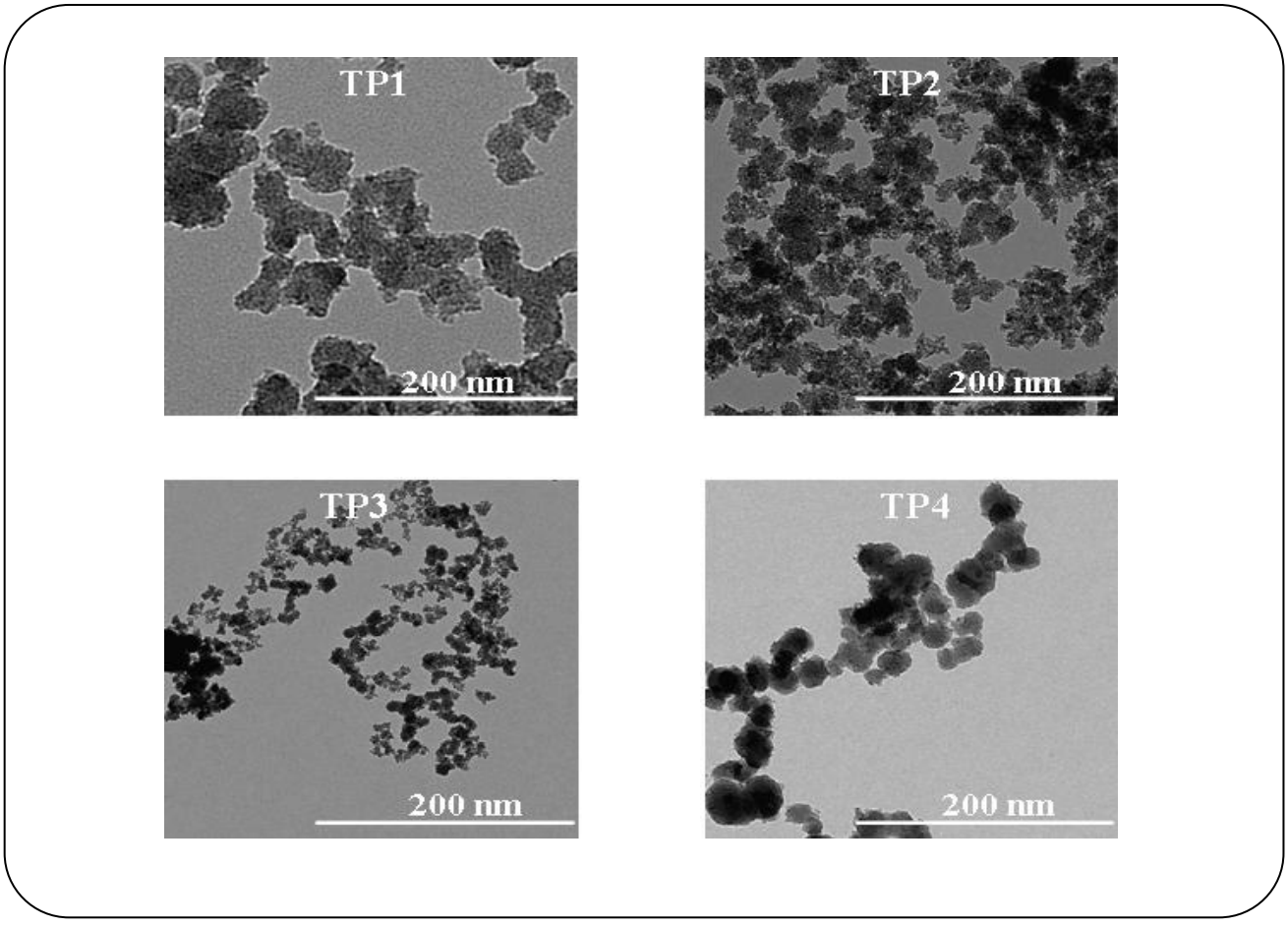

Fig. 1: TEM micrographs of titania nanoparticles TP1 (surfactant: C_{14}TAB), TP2 (surfactant: C_{16}TAB), TP3 (surfactant: C_{18}TAB) and TP4 (surfactant: Plantacare UP K55).

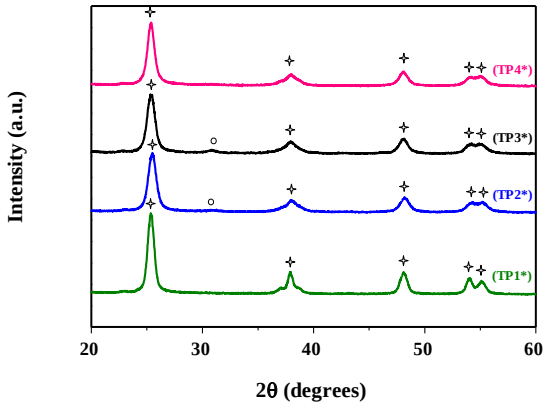

Fig. 2: XRD patterns of TiO_2 nanoparticles after calcination at 450°C: TP1*, TP2*, TP3* and TP4* (Lines marked with a star correspond to anatase, and those marked with a circle correspond to brookite).

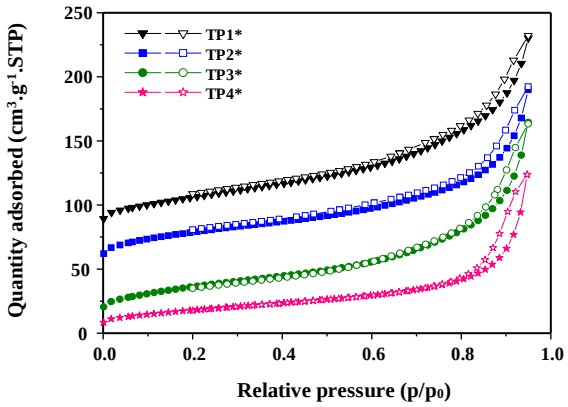

Fig. 3: N_2 adsorption-desorption isotherms of crystallized TiO_2 nanoparticles.

Where S is the crystallite size, λ the wavelength of the X-ray radiation (λ_{Cu}= 0.15406 nm), K a constant taken as 0.94, θ the diffraction angle and *FWHM* is the line width at half maximum height.

The smallest crystallites have been obtained from sample TP3* synthesized by C_{18}TAB with an average size of 10.51 nm (Table 2). The specific surface area and pore size distribution of the as-prepared mesoporous TiO_2 nanoparticles after crystallization were characterized by nitrogen adsorption and desorption isotherms at 77K. The adsorption–desorption isotherms (Fig. 3) of the samples show typical type IV behavior. A hysteresis loop in the adsorption–desorption isotherm was observed at higher pressures ($0.8< P/P_0< 0.95$), indicating the presence of mesoporous structure [37]. Their values of BET surface area (S_{BET}) and average pore diameter of samples are indicated in Table 2. All samples have an important surface area than commercial TiO_2 P25. The highest S_{BET} was presented in TP3*.

Photo-catalytic Degradation of Rhodamine B

The photo-catalytic activities of as-prepared samples were evaluated by monitoring the degradation of RhB solution, where the concentration of RhB is obtained from the linear relation between the absorbance and the concentration of dye solution.

Fig. 3 displays a comparison of photo-catalytic activity for the obtained TiO_2 nanoparticles under UV light. In dark conditions, a decrease of RhB concentration was observed during the first half hour of the test and it was unchanged in the second half hour, indicating that the adsorption equilibrium of dye on catalyst surface was reached. After the dark period, the solution was irradiated with UV light and the reaction started to occur. It is found that all TiO_2 photocatalysts exhibited higher photo-catalytic activity under UV light irradiation than commercial TiO_2 P25. On the contrary the photolysis reaction shows that without TiO_2, RhB decolorization decreases slightly which confirm that as synthesized TiO_2 are effective. The higher photocatalysis process can be related to higher specific surface area [38] and smaller particles [39] because it narrows the band gap of photocatalysts and implies larger contact surfaces exposure to the reagent, which allows photocatalysts to absorb more molecules.

TiO_2 nanoparticles caused decolorization of RhB solutions mainly due to photocatalytic process. Besides all dye solutions were almost completely undergo degradation. Results demonstrated that with the different prepared TiO_2, the decolorization and degradation values were found to be 98.58, 98.72, 99.95 and 98.84% for samples TP1*, TP2*, TP3* and TP4*, respectively. These values were higher than commercial TiO_2 P25 witch was 97.68.

To obtain more detail information about intermediates, and to better comprehend the details of the reaction process, the degradation products were identified by GC/MS and LC/MS. The intermediates were identified on the basis of the information given by the commercial library (NIST 2008). Corresponding to the GC/MS and LC/MS identification, the degradation of RhB can occur via N-de-ethylation and cleavage chromophore. However,

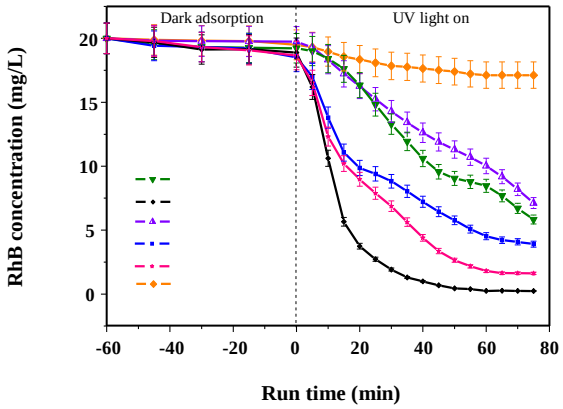

Fig. 4: Photocatalytic decomposition of RhB aqueous solution in presence of Degussa P25 and as synthesized TiO_2 nanoparticles after calcination at 450°C (TP1*, TP2*, TP3* and TP4*).

a peak at *m/z* = 399 was observed indicating possible de-carboxylation of RhB. on the basis of the results, the proposed pathways for the photocatalytic degradation of RhB were depicted in Fig. 5.

Kinetic Study

The kinetics study of photo-catalytic degradation of RhB was studied with pseudo-first-order model according to the approach proposed by *Lente* [40]. The pseudo-first-order model is given as in the following equation:

$$C_t = Xe^{-kt} + E$$

Where *E* is the endpoint, C_t is the concentration of RhB at irradiation time *t* and *k* is a first order rate constant (min^{-1}). The *k* value is an important figure, indicating the photocatalytic performance, and the value is proportional to the photocatalytic activity. The first order rate constant *k* and the coefficient of determination R^2 are given in Table 3. The R^2 values reach the unity indicating that the pseudo-first-order model fits the experimental data quite well. The order of kinetic constants of TiO_2 nanoparticles is *k* (P25)< *k* (TP1*)< *k* (TP2*)< *k* (TP4*) <*k* (TP3*) which confirm that (TP3*) was the perfect sample for the degradation of RhB than the others samples obtained by cationic surfactants and even non ionic template. Besides TP* was more performed than commercial TiO_2 P25.

The higher photocatalytic activity of sample TP3* prepared by cationic surfactant C_{18}TAB is attributed to the homogeneous crystal structure which was beneficial to higher performance rather than anatase and rutile mixed phase in the field of photocatalyst [41]. It was also attributed to the mesoporous structure with large pore size and high surface area caused by surfactant template in the synthesis process [42].

Catalysts re-use studies

It was although appropriate to investigate the re-use of the same photo-catalyst (TP1*, TP2*, TP3* and TP4*) for degradation of a new 20 mg/L RhB dye solution at the same optimum photodegradation conditions determined for the nano-TiO_2. Samples were used after wash and calcinations at 400°C to remove all organic compounds. The obtained nanoparticles were named (TP1**, TP2**, TP3** and TP4**). After the second use, the photocatalytic activity of TiO_2 nanoparticles is decreased but it still important and the disappearance of the organic molecule follows a pseudo first kinetic order model. However, the degradation time was increased from 75 min to 135 min to achieve maximum photo-degradation. It was also observed that sample TP3** showed the higher RhB photodegradation than the others.

CONCLUSIONS

In summary, the mesoporous TiO_2 prepared via the fast sol–gel method by introducing different surfactants as the template exhibits smaller grain size and much larger surface area with spherical morphology. After calcination, the XRD pattern indicates the presence of crystalline anatase phase TiO_2 for all samples. The as synthesized nano TiO_2 nanostructures exhibited good photo-catalytic activity for the degradation of RhB dye under UV light even after the second use. When the sample is prepared with cationic surfactant C_{18}TAB, it has a small crystallite size with large pore size and high surface area witch make it better in photocatalysis than the others samples obtained by C_{14}TAB, C_{16}TAB and the nonionic surfactant. Moreover, the possible photocatalytic degradation pathway of RhB was proposed and the major intermediates were identified by GC/MS technique. It was proposed that the decomposition of RhB occurred via competitive pathways, the chromophore cleavage, decarboxylation and the N-deethylation. All ways happened concurrently and

Table 3: Kinetics parameters of photodegradation of rhodamine B onto TiO_2 samples according to pseudo-first-order.

Sample	k (min^{-1})	R^2
TP1*	0.00877	0.9814
TP2*	0.03532	0.9876
TP3*	0.07265	0.9816
TP4*	0.03686	0.9932
P25	0.00452	0.9968

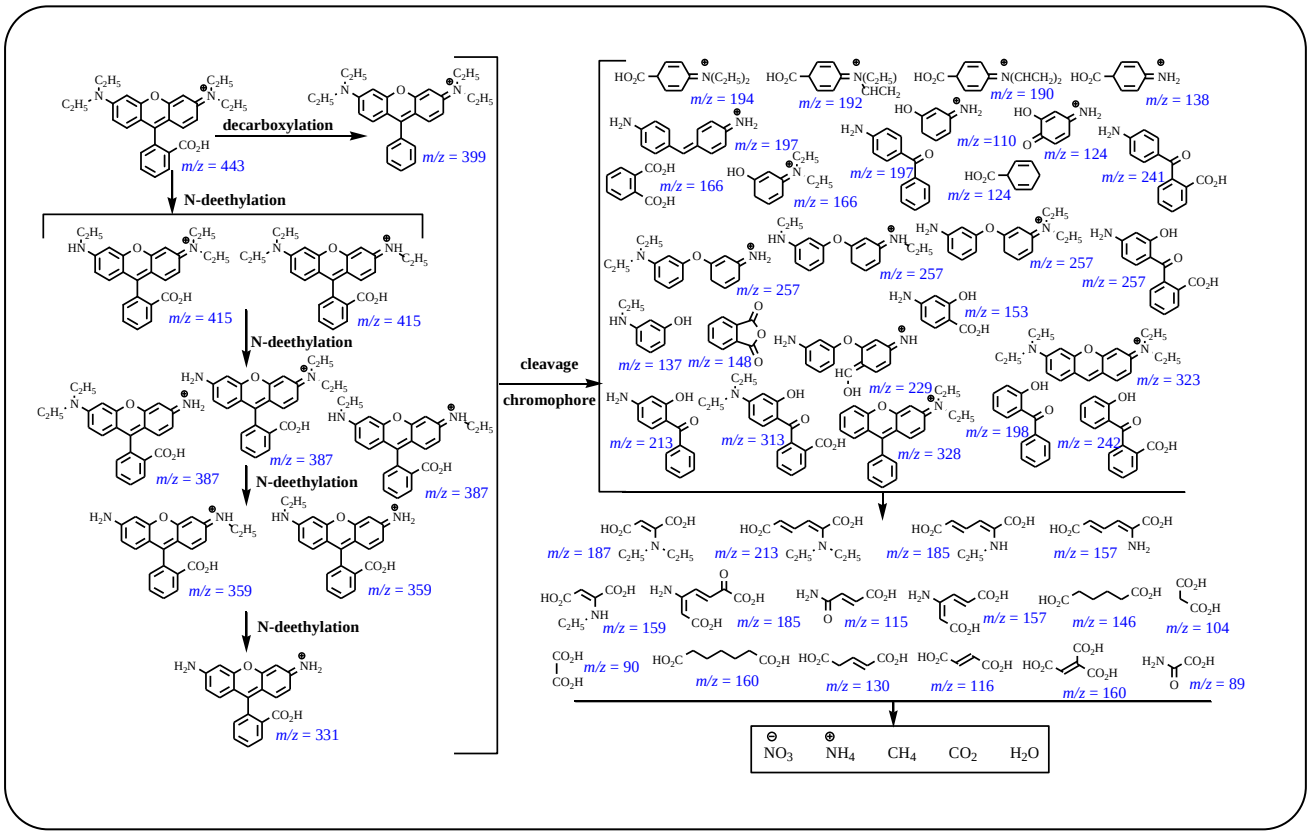

Fig. 5: Proposed mechanism of photocatalytic degradation of RhB using TiO_2 nanoparticles under UV light irradiation.

may lead the RhB molecule toward acid molecules that will be mineralized later to NH_4^+, NO_3^-, CH_4, H_2O, and CO_2.

Acknowledgements

We greatly acknowledge the financial support of the Ministry of Higher Education and Scientific Research of Tunisia.

Received : Jul. 10, 2017 ; Accepted : Jan. 1, 2018

REFERENCES

[1] Chen X., Kuo D.H., Lu D., Hou Y., Kuo Y.R., Synthesis and Photocatalytic Activity of Mesoporous TiO_2 Nanoparticle Using Biological Renewable Resource of un-Modified Lignin as a Template, *Microporous Mesoporous Mater.*, **223**: 145–151 (2016).

[2] Lee K.W., Kim M., Kim J.M., Kim J.J., Lee I.H., Enhanced Photovoltaic Performance of Back-Illuminated Dye-Sensitized Solar Cell Based on TiO_2 Nanoparticle/Nanowire Composite Film in Cobalt Redox System, *J. Alloys Compd.*, **656**: 568–572 (2016).

[3] Khan S.A., Ali S., Sohail M., Morsy M.A., Yamani Z.H., Fabrication of $TiO_2/Ag/Ag_2O$ Nanoparticles to Enhance the Photocatalytic Activity of Degussa P25 Titania, *Aust. J. Chem.*, **69**: 41–46 (2016).

[4] Usha K., Mondal B., Sengupta D., Das P., Mukherjee K., Kumbhakar P., Development of Multilayered Nanocrystalline TiO_2 Thin Films for Photovoltaic Application, *Opt. Mater.*, **36**: 1070–1075 (2014).

[5] Lin L.Y., Ye M.H., Tsai K.W., Chen C.Y., Wu C.G., Ho K.C., Highly Ordered TiO_2 Nanotube Stamps on Ti Foils: Synthesis and Application for All Flexible Dye–Sensitized Solar Cells, *Electrochem. Commun.*, **37**: 71–75 (2013).

[6] Ruiz A.M., Sakai G., Cornet A., Shimanoe K., Morante J.R., Yamazoe N., Microstructure Control of Thermally Stable TiO_2 Obtained by Hydrothermal Process for Gas Sensors, *Sens Actuator B-Chem.*, **103**: 312–317 (2004).

[7] Zhao L., Liu Y., Wang L., Zhao H., Chen D., Zhong B., Wang J., Qi T., Production of Rutile TiO_2 Pigment from Titanium Slag Obtained by Hydrochloric Acid Leaching of Vanadium-Bearing Titanomagnetite, *Ind. Eng. Chem. Res.*, **53**: 7 0–77 (2014).

[8] Chen X., Mao S.S., Titanium Dioxide Nanomaterials: Synthesis, Properties, Modifications, and Applications, *Chem. Rev.*, **107**: 2891–2859 (2007).

[9] Yang H.G., Liu G., Qiao S.Z., Sun C.H., Jin Y.G., Smith S.C., Zou J., Cheng H.M., Qing G., Lu M., Solvothermal Synthesis and Photoreactivity of Anatase TiO_2 Nanosheets with Dominant {001} Facets, *J. Am. Chem. Soc.*, **131**: 4078–4083 (2009).

[10] Pookmanee P., Phiwchai I., Yoriya S., Puntharod R., Phanichphant S., Titanium Dioxide (TiO_2) Nanopowder Prepared by the Low Temperature Solvothermal Method, *Ferroelectrics*, **457**: 30–38 (2013).

[11] Kim C.S., Moon B.K., Park J.H., Chung S.T., Son S.M., Synthesis of Nanocrystalline TiO_2 in Toluene by a Solvothermal Route, *J. Cryst. Growth*, **254**: 405–410 (2003).

[12] Xie M., Jing L., Zhou J., Lin J., Fu H., Synthesis of Nanocrystallineanatase TiO_2 by One-Pot Two-Phase Separated Hydrolysis-Solvothermal Processes and Its High Activity for Photocatalytic Degradation of Rhodamine B, *J. Hazard. Mater.*, **176**: 139–145 (2010).

[13] Nian J.N., Teng H., Hydrothermal Synthesis of Single-Crystalline Anatase TiO_2 Nanorods with Nanotubes as the Precursor, *J. Phys. Chem. B*, **110**: 4193–4198 (2006).

[14] Wu J.M., Tang M.L., Hydrothermal Growth of Nanometer- to Micrometer-size Anatase Single Crystals with Exposed (001) Facets and Their Ability to Assist Photodegradation of Rhodamine B in Water, *J. Hazard. Mater.*, **190**: 566–573 (2011).

[15] Asilturk M., Sayılkan F., Erdemoglu S., Akarsu M., Sayılkan H., Erdemoglu M., Arpac E., Characterization of the Hydrothermally Synthesized Nano-TiO_2 Crystallite and the Photocatalytic Degradation of Rhodamine B, *J. Hazard. Mater. B*, **129**: 164–170 (2006).

[16] Sarkar B., Singhal N., Goyal R., Bordoloi A., Konathala L.N.S., Kumar U., Bal R., Morphology-Controlled Synthesis of TiO_2 Nanostructures for Environmental Application, *Catalysis Commun.*, **74**: 43–48 (2016).

[17] Guimaraes J.L., Abbate M., Betim S.B., Alves M.C.M., Preparation and Characterization of TiO_2 and V_2O_5 Nanoparticles Produced by Ball-Milling, *J. Alloys Compd.*, **352**: 16–20 (2003).

[18] Gu D., Wang B., Zhu Y., Wu H., Photocatalytic Degradation of Gaseous Formaldehyde by Modified Hierarchical TiO_2 Nanotubes at Room Temperature, *Aust. J. Chem.*, **69**: 343–348 (2016).

[19] Meher S.R., Balakrishnan L., Sol–Gel Derived Nanocrystalline TiO_2 Thin Films: Apromising Candidate for Self-Cleaning Smart Window Applications, *Mater. Sci. Semicond. Process*, **26**: 251–258 (2014).

[20] Liu B., Zeng H.C., Fabrication of ZnO "Dandelions" via a Modified Kirkendall Process, *J. Am. Chem. Soc.*, **126**: 16744–16746 (2004).

[21] Adraider Y., Pang Y.X., Sharp M.C., Hodgson S.N., Nabhani F., Al-Waidh A., Fabrication of Titania Coatings on Stainless Steel *Via* Laser-Induced Deposition of Colloidal Titanium Oxide from Sol-Gel Suspension, *Mater. Chem. Phys.*, **138**: 245–252 (2013).

[22] Li H., Zhao G., Chen Z., Song B., Han G., TiO_2–Ag Nanocomposites by Low-Temperature Sol–Gel Processing, *J. Am. Ceram. Soc.*, **93**: 445–449 (2010).

[23] Maheswari D., Venkatachalam P., Fabrication of High Efficiency Dye-Sensitised Solar Cell with Zirconia-Doped TiO_2 Nanoparticle and Nanowire Composite Photoanode Film, *Aust. J. Chem.*, **68**: 881–888 (2015).

[24] Elghniji K., Saad M., Araissi M., Elaloui E., Moussaoui Y., Chemical Modification of TiO_2 by $H_2PO_4^-/HPO_4^{2-}$ Anions Using the Sol-Gel Route with Controlled Precipitation and Hydrolysis: Enhancing Thermal Stability, *Mater. Sci. Poland.*, **32**: 617–625 (2014).

[25] Gong X., Wang H., Yang C., Li Q., Chen X., Hu J., Photocatalytic Degradation of High Ammonia Concentration Wastewater by TiO_2, *Futur Cities Environ.*, **1**: 12- (2015).

[26] Oseghe E.O., Ndungu P.G., Jonnalagadda S.B., Synthesis of MesoporousMn/TiO_2 Nanocomposites and Investigating the Photocatalytic Properties in Aqueous Systems, *Environ. Sci. Pollut. Res.*, **22**: 211–222 (2015).

[27] Antonelli D.M., Ying Y.J., Synthesis of Hexagonally Packed Mesoporous TiO_2 by a Modified Sol–Gel Method, *Angew. Chem. Int. Ed. Engl.*, **34**: 2014–2017 (1995).

[28] Yang H.G., Zeng H.C., Preparation of Hollow Anatase TiO_2 Nanospheres via Ostwald Ripening, *J. Phys. Chem. B*, **108**: 3492–3495 (2004).

[29] Ren T.Z., Yuan Z.Y., Su B.L., Surfactant-Assisted Preparation of Hollow Microspheres of Mesoporous TiO_2, *Chem. Phys. Lett.*, **374**:170–175 (2003).

[30] Cui W., Shao M., Liu L., Liang Y., Rana D., Enhanced Visible-Light-Responsive Photocatalytic Property of PbS-Sensitized $K_4Nb_6O_{17}$ Nanocomposite Photocatalysts, *Appl. Surf. Sci.*, **276**: 823–831 (2013).

[31] Bakre P.V., Volvoikar P.S., Vernekar A.A., Tilve S.G., Influence of Acid Chain Length on the Properties of TiO_2 Prepared by Sol-Gel Method and LC-MS Studies of Methylene Blue Photodegradation, *J. Colloid Inter. Sci.*, **474**: 58–67 (2016).

[32] Rhouta B., Bouna L., Maury F., Senocq F., Lafont M.C., Jada A., Amjoud M., Daoudi L., Surfactant-Modifications of Na^+-Beidellite for the Preparation of TiO-Bd Supported Photocatalysts: I-Organobeidellite Precursor for Nanocomposites, *Appl. Clay Sci.*, **115**: 260–265 (2015).

[33] Wang X., Hao J., Ionogels of Sugar Surfactant in Ethylammonium Nitrate: Phase Transition from Closely Packed Bilayers to Right-Handed Twisted Ribbons, *J. Phys. Chem. B*, **119**: 13321–13329 (2015).

[34] International Union of Pure and Applied Chemistry., Reporting Physisorption Data for Gas/Solid Systems with Special Reference to the Determination of Surface Area and Porosity, *Pure Appl. Chem.*, **87**: 603–619 (1957).

[35] Zhang H., Banfield J.F., Understanding Polymorphic Phase Transformation Behavior During Growth of Nanocrystalline Aggregates: Insights from TiO_2, *J. Phys. Chem. B*, **104**: 3481–3487 (2000).

[36] Oskam G., Nellore A., Penn R.L., Searson P.C., The Growth Kinetics of TiO_2 Nanoparticles from Titanium (IV) Alkoxide at High Water/ Titanium Ratio, *J. Phys. Chem. B*, **107**: 1734–1738 (2003).

[37] Liu E.Q., Guo X.L., Qin L., Shen G.D., Wang X.D., Fabrication and Photocatalytic Activity of Highly Crystalline Nitrogen Doped Mesoporous TiO_2, *Chin. J. Catal.*, **33**: 1665–1671 (2012).

[38] Cui W., Guo D., Liu L., Hu J., Rana D., Liang Y., Preparation of $ZnIn_2S_4$ / $K_2La_2Ti_3O_{10}$ Composites and Their Photocatalytic H_2 Evolution from Aqueous Na_2S / Na_2SO_3 under Visible Light Irradiation, *Cat Comm.*, **48**: 55–59 (2014).

[39] Cui W., Qi Y., Liu L., Rana D., Hu J., Synthesis of PbS – $K_2La_2Ti_3O_{10}$ Composite and Its Photocatalytic Activity for Hydrogen Production, *Prog. Nat. Sci. Mater. Int.*, **22**: 120–125 (2012).

[40] Lente G., "Deterministic Kinetics in Chemistry and Systems Biology", Springer, pp. 125-126 (2015).

[41] Park J.H., Jang I., Song K., Oh S.G., Surfactants-Assisted Preparation of TiO_2-Mn Oxide Composites and Their Catalytic Activities for Degradation of Organic Pollutant, *J. Phys. Chem. Solids*, **74**: 1056–1062 (2013).

[42] He K., Zhao C., Zhao G., Han G., Effects of Pore Size on the Photocatalytic Activity of Mesoporous TiO_2 Prepared by a Sol–Gel Process, *J. Sol-Gel Sci. Technol.*, **75**: 557–563 (2015).